*Manuscript
Click here to view linked References

# APPLICATION OF ABS MEMBRANES IN DYNAMIC FILTRATION FOR *CHLORELLA SOROKINIANA* DEWATERING

M. Hapońska[a], E. Clavero[b], J. Salvadó[a,b] , C. Torras[b,✉]

[a]Departament d'Enginyeria Química, Universitat Rovira i Virgili, Av. Països Catalans 26, 43007 Tarragona, Catalonia, Spain.

[b]Catalonia Institute for Energy Research, IREC, Marcel·lí Domingo 2, 43007 Tarragona, Catalonia, Spain.

✉Corresponding author: ctorras@irec.cat, carlestorrasfont@gmail.com, Tel. 00.34.977.202.444

## ABSTRACT

This work focuses on the use of dynamic membrane filtration with cheap membranes manufactured from acrylonitrile butadiene styrene polymer for dewatering of *Chlorella sorokiniana* microalgae strain.

Dynamic filtration based on vibration was used at pilot scale and compared to conventional cross-flow filtration to demonstrate how fowling can be greatly minimized. Experiments were carried-out with different types of commercial membranes from different pore sizes and materials such as polyethersulfone or polyacrylonitrile.

ABS membranes were produced, characterized (scanning electron microscopy, contact angle and porosity measurements) and tested with conventional and dynamic filtration. Composition of acrylonitrile butadiene styrene polymeric solution as well as conditions of membrane preparation were examined in order to obtain a useable membrane for microalgae filtration. Acrylonitrile butadiene styrene membranes offered promising results in terms of permeability when applied to both filtration techniques for *Chlorella sorokiniana* dewatering. The influence of different concentrations of microalgae culture as a feed for dynamic membrane filtration was examined. To confirm total microalgae rejection the optical density of feed, permeate and retentate was studied in all experiments.

Acrylonitrile butadiene styrene material is order of magnitudes cheaper than conventional membrane materials. Combined with dynamic filtration, both may turn membrane filtration into a preferred technology for microalgae dewatering.

**Keywords:** acrylonitrile butadiene styrene; membrane; microalgae; dewatering; dynamic filtration

## List of abbreviations

ABS – acrylonitrile butadiene styrene

CA – contact angle

DMA – N,N-dimethylacetamid

IPA - isopropanol

MF – microfiltration

MWCO – molecular weight cut-off

NMP – 1-methyl-2-pyrrolidinone

OD – optical density

PAN – polyacrylonitrile

PES – polyethersulfone

SEM – scanning electron microscope

UF – ultrafiltration

VSEP – vibratory shear enhanced process

# 1 INTRODUCTION

Finding an alternative for nonrenewable energy sources became the objective of extensive studies. Because of its advantages over conventional fuels, its sustainability, biodegradability and suitability to use in existing diesel engines, biodiesel seems to be a proper substitute for petroleum diesel [1,2]. Microalgae with their unicellular structure can efficiently turn solar into chemical energy. Due to their ability to capture carbon dioxide, fast growth rate and high content of lipids, carbohydrates and proteins are considered as a competitive material for various industrial purposes [3,4]. They are being commonly used in the production of nutraceuticals, pharmaceuticals, cosmetics, fine chemicals and to provide fuel [5,6]. Although the idea of using microalgae as a feedstock for biofuel production has been proposed in the 50s, in recent years they became a highly considered alternative for fossil fuels. However, costs of the overall process need to be decreased.

In comparison with plant crops, microalgae have higher biomass productivity and lower cost per yield [7]. They have a very short harvesting time and require much less land area for cultivation than terrestrial plants. Moreover, they are capable of growing in more radical conditions, from fresh water up to extremely saline water. The cultivation of microalgae in sea water, which is inapplicable in agriculture, reduces the demand of fresh water consumption [8]. Regardless of the numerous advantages of using microalgae as a staple for biofuel production, the overall process still needs to be improved in order to reduce the production costs in the industrial scale [9]. Since a high volume of microalgae is processed and implies a considerable cost, dewatering becomes a critical step to be optimized. Techniques commonly used for harvesting are flocculation / sedimentation [10], flotation [11], centrifugation [12] and filtration. The flocculation/sedimentation process refers to the aggregation of microalgae in a suspension to form masses that subsequently can settle. Even if flocculation reduces the need of energy intensive separation mechanisms, the concentration obtained is low (< 10 % of solids content) [13] and needs further concentration using other methods, like centrifugation. Even though centrifugation is more effective, the shear forces can disrupt microalgae cells and it is high energy demanding, which results in substantial operational costs. For those reasons, filtration is a promising technique [14,15]. Microalgae cell size allows for the application of membrane micro/ultrafiltration (MF/UF) for the dewatering purpose. The list of benefits in using membranes includes no chemical additives, simplicity in operation and low energy consumption [16]. For the dewatering purpose, both polymeric and ceramic membranes can be used. Although ceramic membranes offer good performances in terms of flow and reproducibility, they are much more expensive than polymeric ones [17]. Recent studies showed that membranes produced from cheap polymers, such as ABS, are promising materials which could be applied in the dewatering step for microalgae biorefining [18]. Therefore, when using those cheaper membranes, a significant reduction in the costs of the overall process can be obtained.

The main disadvantage in microalgae MF/UF is fouling [17]. Filtration of biological feeds results in additional difficulties due to the compressibility of the mass formed. Another factor that has a significant influence on the membrane performance is the increase in the feed concentration. In conventional cross-flow filtration, cake formation over the membrane surface and pore-blocking can result in up to 99% permeability reduction. Previous studies showed that fouling issues can be minimized by using dynamic filtration, which increases turbulence and raises shear stress over the membrane surface [19]. There are several types of commercially available dynamic filtration systems, like rotating cylindrical membranes, rotating disk systems and vibrating systems [20]. Vibratory shear enhanced process (VSEP) was already successfully applied for the purification of drinking water, skim milk ultrafiltration, pervaporation as well as for baker's yeast microfiltration [21]. It was also found to be a proper technique for microalgae dewatering [22,23]. However, so far only commercial membranes have been used in the microalgae filtration experiments with VSEP.

When compared to other polymers, ABS is up to three orders of magnitude cheaper. Depending on the market, PES costs vary between 432 \$ kg$^{-1}$ (GoodFellow) and 480 \$ kg$^{-1}$ (Sigma Aldrich), PAN 375 \$ kg$^{-1}$ (GoodFellow) and 1,850 \$ kg$^{-1}$ (Sigma Aldrich), and ABS price is only 2.4 \$ kg$^{-1}$ (Plasticker) [18]. ABS polymers are highly resistant, have good thermal stability and durability [24]. Due to their properties and low price, they are being commonly used in packaging industry, for toy production as well as for 3D printing [25–27]. Although this material is so ubiquitous in everyday life, it is not so common in membrane industry. Some research with ABS membranes can be found in gas permeation studies [28–30]. Preliminary studies with filtration of *Phaeodactylum tricornutum* were performed for ABS synthesized membranes, however only conventional cross-flow technique was used for this purpose [18].

The main aspect considered in this work was to combine vibrating filtration method with new cheap membrane materials for the dewatering of microalgae. *Chlorella sorokiniana* was used in dewatering with both conventional and dynamic filtration modules.

## 2 MATERIALS AND METHODS

### 2.1 Microalgae biomass

Experiments were carried out with the freshwater microalgae *Chlorella sorokiniana* Shihira & R.W.Krauss (strain CCAP 211/8K), a 2-5 µm spherical to ellipsoidal freshwater green unicellular alga. Dynamic filtration was performed with 300 L cultures whereas cross flow filtration was conducted with material from either 300 L cultures or 4 L cultures. Cultures were illuminated (16:8 light: dark cycle) with cool daylight fluorescents and kept at 24±2.5 °C. Four litre cultures were grown in five litre flasks (18 cm in diameter) with BBM3N3S medium [31] and aerated with air with 0.5% $CO_2$. They were illuminated with OSRAM L30W/865 fluorescents, which gave irradiance on the flask's surface of 200 µmol photon $m^{-2}$ $s^{-1}$. 300 L cultures were grown in column photobioreactors (50 cm diam.) with tap water enriched with the following nutrients (in g $m^{-3}$): $NaNO_3$ ($5.00\cdot 10^{-4}$), $K_2HPO_4.3H_2O$ ($2.10 \cdot 10^{-5}$), $KH_2PO_4$ ($3.75\cdot 10^{-5}$), $Na_2EDTA$ ($1.67\cdot 10^{-5}$), $FeCl_3$. $6H_2O$ ($4.84\cdot 10^{-6}$), $ZnSO_4\cdot 7H_2O$ ($4.85\cdot 10^{-7}$), $MnCl_2\cdot 4H_2O$ ($8.87\cdot 10^{-7}$), $Na_2MoO_4.2H_2O$ ($2.46\cdot 10^{-8}$), $CuSO_4\cdot 5H_2O$ ($4.31\cdot 10^{-8}$) and $CoCl_2\cdot 6H_2O$ ($1.37\cdot 10^{-8}$). Cultures were aerated with air and illuminated with Philips MASTER TLD 58W/865 giving irradiance on the photobioreactor surface of 300 µmol photon $m^{-2}$ $s^{-1}$. For the tests with concentrated microalgae biomass, retentate obtained from the vibratory dewatering of original culture was collected and used as a feed for further experiments.

### 2.2 Membranes

Experiments were performed with commercially available polymeric membranes and synthesized ones. The filtration area was 139 $cm^2$ for conventional cross-flow filtration module and 446 $cm^2$ for dynamic filtration module. In order to ensure total microalgae rejection, the main criterion for membrane selection was the molecular weight cut-off (MWCO), chosen according to *Chlorella sorokiniana* cell size. Commercial membranes PES5 (polyethersulfone, MWCO 7,000 Da), PAN50 (polyacrylonitrile, 50,000 Da) and PES20 (polyethersulfone, 200,000 Da) produced by Sepro were purchased from New Logic (United States).

For the synthesis of non-commercial membranes N,N-Dimethylacetamid, DMA (≥99.5%, CAS 127-19-5), 2-Propanol, IPA (≥99.8%) and 1-Methyl-2-pyrrolidinone, NMP (anhydrous, 99.5%, CAS 872-50-4) were purchased from Sigma-Aldrich (Spain). Acetone, for synthesis (BP, USP) was purchased from LABKEM (Spain). ABS copolymer Novodur P2H-AT NR, kindly delivered by Styrolution (Spain), was employed with a density of 1050 kg m$^{-3}$, processing temperature between 230 and 260$^{o}$C and tensile stress at yield of 44 MPa.

## 2.2 Methods

### 2.2.1 Membrane synthesis

Polymeric membrane synthesis was performed via phase inversion precipitation with several polymer/solvent systems and different non-solvents in coagulation bath (Table 1).

The polymer and the solvent were mixed and stirred using magnetic stirrer at room temperature for 72 h to obtain a homogenous polymeric solution. Afterwards, the solution was left for at least 24 h in order to remove all the bubbles from the bulk. The solution was deposited onto a glass plate using a casting knife with an adjustable thickness gap regulated by an incorporated micrometer. In all cases, the casting knife gap was adjusted to 200 µm, except for M5, where the gap thickness applied was 300 µm. It was necessary to obtain the membrane with good mechanical properties for the incorporation in the vibratory system. The casting knife was set in motion by an automatic film applicator with a constant traverse speed of 50 mm s$^{-1}$ (BYK – Gardner Automatic Film Applicator). Immersion of the cast polymeric solution into a coagulation bath caused phase inversion precipitation, which resulted in the formation of a thin film. The temperature of the coagulation bath was fixed to 20 $^{o}$C, ± 5 $^{o}$C, except for M5, where the temperature was fixed to 50 $^{o}$C, ± 5 $^{o}$C, in order to produce a membrane applicable for use with dynamic filtration module.

### 2.2.2 Membrane morphology

Scanning electron microscope (SEM, JEOL JSM-6400 Scanning Microscopy Series with working voltage of 20kV) was used to study the cross-section and the surface of membranes. Samples were immersed first into ethanol, and afterwards into liquid nitrogen for freezing. This procedure allowed the membrane to be broken preserving the internal porous structure. Next, deposition of gold layer over the samples was performed using sputtering in order to induce conductive properties [32]. Porosity of materials was analyzed based on SEM images using  membrane SEM micrographs interpretation software IFME [33].

### 2.2.3 Contact Angle

Sessile drop technique with automatic video-based analysis system OCA 35 (Dataphysics) was used to measure membranes contact angles (CA). Usually, the droplet reached a steady state on a membrane surface around 30 s after dispensing. At least five measurements were performed for each membrane.

### 2.2.4 Permeability

The initial permeability of membranes was determined by water flux measurements. After that the filtration of microalgae biomass was performed. At the end, permeability for water was measured after cleaning the system. The last step allowed us to determine the irreversible fouling resistance of membranes. In the case of conventional cross-flow filtration distilled water was always used and for the experiments with vibrating set-up tap water instead of distilled water was used. This procedure in terms of water usage needed to be adjusted to the size of equipment and to the volume of liquid processed.

### 2.2.5 Optical density

Optical density (OD) was calculated from the results of absorbance measurements for feed, permeate and concentrate of microalgae dewatering. Absorbance was measured using a microplate reader (INFINITE M200 PRO, Tecan).

Absorbance was always read at concentrations in which the relation between absorbance and concentration maintained linearity. Therefore, if necessary, samples were adjusted to an absorbance below 0.4 and the resulting absorbance of the diluted sample was multiplied by the dilution factor. Finally, the absorbance data obtained from 96 well plates (path length of 0.5052 cm) were converted to OD values.

## 2.3 Equipment

Experiments were carried out using two filtration setups. (Fig. 1) In the cross-flow filtration, microalgae culture was placed in the temperature-controlled recirculation tank (cooled using Refrigerated Heating Bath with air-cooled refrigerating unit, Huber, K6-cc-NR) and pumped by a screw pump towards a membrane cell system (SEPA CFII, GE Osmonics). A transmembrane pressure was regulated with a compact back pressure regulator and a volumetric flow meter. The retentate was returned from the membrane module to the recirculation tank, while permeate was collected in the permeation tank placed over the scale. The scale was connected to a computer in order to read the actual mass of permeate during the experiment and to calculate the actual mass flow rate in a five-second frequency.

Transmembrane pressure was fixed at 350 kPa and recirculating flow rate at 50 L $h^{-1}$. The volume of microalgae culture used as the feed was 2 L.

Dynamic membrane filtration of microalgae culture was performed using Vibratory Shear Enhanced Processing (VSEP, series L, New Logic Research, Inc.) system. Detailed description of this setup can be found elsewhere [34].

Vibrational frequency applied was 55.4 ± 0.1 Hz, recirculating flow rate was equal to 570 ± 5 L $h^{-1}$ and the transmembrane pressure was fixed at 350 kPa. The microalgae volume used with the VSEP was 38 L when original culture was filtered and 15 L for the dewatering of concentrated biomass.

# 3. RESULTS AND DISCUSSION

## 3.1 Membrane characterization

### 3.1.1 Morphology – scanning electron microscopy micrographs

Cross-section micrographs of commercial and synthesized materials provided information about membranes morphology (Fig. 2). All commercially available membranes showed a similar structure with big macrovoids. PES5 and PAN50 membranes had several types of macrovoids throughout the membrane thickness. Big vertical macrovoids were found in the whole membrane matrix, while smaller macrovoids were also present near the membrane top side (the selective). PES20 membrane did not exhibit the latter near the selective surface.

On the contrary, synthesized ABS membranes had sponge-like morphology with smaller and enclosed macrovoids inside the structure compared with the commercial membranes. M4 contained bigger pores than M5 as a consequence of different temperatures of the coagulation bath applied. A higher temperature of the coagulation bath resulted in a slower phase inversion precipitation and in the formation of a denser structure.

In all cases, a dense top layer was observed. It ensured total microalgae rejection in the dewatering experiments.

The results of porosity measurements of all membranes are presented in Table 2. Because of the presence of macrovoids commented above, commercial membranes were more porous than ABS synthesized ones. PES5 was the membrane with the greatest value of porosity within all tested materials. Thus we expected that commercial membranes would exhibit greater permeability than the synthesized ones, which were not optimized.

As regards of synthesized membranes, an important factor that was also considered was its mechanical behavior. Membranes not only need to separate desired compounds with the highest possible flow rate, but also need to be mechanically stable. A main non-desirable behavior encountered when producing ABS membranes was its brittle performance. It was found that coagulation bath temperature influenced significantly this property. By increasing the temperature, significantly less brittle membranes were obtained. Therefore, M5 membrane produced in a coagulation bath with a temperature of 50 ºC was mechanically better than that obtained with a temperature of 20 ºC. Mechanical properties were not measured in this study but references can be found elsewhere [18].

### 3.1.2 Contact angle

Contact angle values measured for commercial and synthesized membranes are summarized in Table 2. It can be observed that all the materials gave values lower than $90^{o}$, which indicated hydrophilic properties of the surface, strongly desired for the dewatering purpose. The smaller the contact angles, the better the hydrophilicity of the membrane is [35]. Nevertheless, PES membranes offered values very close to the theoretical limit.

Concerning commercial membranes, polyethersulfone materials, PES5 and PES20, with CA values greater than 85° were more hydrophobic when compared to polyacrylonitrile one (PAN50) with CA lower than 60°. This result indicated that PAN50 was offering the best properties of permeability with water, which was confirmed by tests performed before microalgae sludge filtration (Table S1 and Table S2). In fact, one of the main advantages of PAN material is its hydrophilic property although it is one of the most expensive materials within the common polymeric membrane materials family. It should be considered that, in this case, cost reduction is one of the main targets, so PAN material is useful for technical reference but not for this industrial application.

For synthesized ABS membranes, M4 had greater values of contact angle than M5. It means that a higher temperature of coagulation bath results in better hydrophilicity of the surface. Moreover, the contact angle value of the M5 membrane was the closest one to that of the most hydrophilic commercial membrane, PAN50. Therefore, another advantage of ABS material is its clear hydrophilic behavior, closer to PAN material than others like polysulfone or polyethersulfone but much cheaper than all of them.

## 3.2 Filtration experiments

### 3.2.1 Conventional cross-flow filtration

Figure 3 shows the permeabilities obtained with all the membranes tested in the conventional setup. The results include permeability measurement with water of the virgin membrane and after the experiment. It allows comparing initial membrane performance as well as irreversible fouling. Also, permeability with the microalgae sludge is presented. Additionally, in supplementary material, Table S1 can be found with numerical values.

The membrane that exhibited larger water permeability was PES20, followed by PAN50 and PES5. A large difference between the last one and others is according to their MWCO. Synthesized membranes (M4, M5) offered less water permeability due to their non-optimized synthesis (i.e. less porosity than commercial membranes) as explained above.

Concerning the microalgae sludge permeability, results showed a severe fouling when using commercial membranes, especially with PAN50 and PES20 membranes. The PES5 ultrafiltration membrane, with the lowest MWCO, exhibited a permeability value between those obtained for the other two membranes. This implied that the volumetric flow reduction (ratio between the microalgae and water permeability) was much less in this membrane than in the others and therefore, it corresponded to the membrane with less fouling (78% for PES5, 95% for PAN50 and 93% for PES20). Although the microfiltration range would be enough to reject microalgae, ultrafiltration membrane offered better performance due to the less fouling. Nurra [22], Zhang [36] and Tansel [37] in their studies reported fouling formation due to the different pore size of membranes thereby pointing in the same direction. Considering our own synthesized membranes, results showed that despite their water permeabilities being much lower than for commercial membranes, microalgae permeabilities were closer. Volumetric flow reduction was 41% for M4 and 89% for M5. Therefore, in both cases, this value was lower than for commercial membranes. In absolute terms, although microalgae permeability was higher for commercial membranes, M5 membrane offered a microalgae permeability that was only half of the PAN50 one (best case). This result is promising considering that the synthesized membranes were not optimized and that the price of ABS material is three orders of magnitude lower than PAN material.

The measurement of water permeability after performing the experiment and cleaning the system (including the membrane) allowed determining the irreversible fouling. The membrane with higher irreversible fouling was PES20. The ratio between water permeability before and after the experiment was 81%. The other membranes exhibited similar behavior, including synthesized membranes, with ratios lower than 36%.

From among the synthesized membranes tested, a better permeability for water as well as for microalgae filtration was obtained with M5 membrane. For this reason and because of better mechanical resistance, it was chosen in order to be tested in dynamic filtration experiments.

### 3.2.2 Dynamic filtration

Figure 4 shows the permeabilities obtained with all the membranes tested in the vibrational setup. The results include water permeability measurement with the virgin membrane and then after the experiment. Also, permeability with the microalgae sludge is presented. Numerical values are presented in Table S2.

In terms of water permeability for vibrating filtration, the highest values were obtained with PAN50 membrane. Water permeability for PES20 decreased when compared to the results obtained with cross-flow filtration (Fig. 3 and Fig. 4), likely due to dis-homogeneities of the membrane. Again, water permeability differences between commercial membranes were those expected due to their MWCO and porosity. For the synthesized membrane, water permeability was also lower for the same reasons explained in the case of conventional filtration.

Regarding microalgae permeability, the most noticeable result was that performance was in all cases much higher in dynamic filtration than in conventional. The ratio between permeabilities ranged from 1.5 for M5 membrane up to 4 for PES5 membrane. A ratio of 4 not only indicated a technical improvement of the process but also an economic one considering that the plus of energy added in the system for vibration represents approximately only 10% of the pumping cost. Comparing the performance of the commercial membranes with this technology, results showed that the membrane with less MWCO (PES5) still improved the operation, as it was the one with the highest permeability ($4.2 \cdot 10^{-7}$ m $h^{-1}$ $Pa^{-1}$). For PES5 and M5 membranes, results showed that permeability with microalgae sludge was close to permeability with water (low volumetric flow reductions).

To assess irreversible fouling, permeability with water before and after the experiment was considered (the system was cleaned before measuring permeability with water after the experiment). Results showed that, also in this aspect, dynamic filtration enabled a decrease on irreversible fouling by reducing the cake formation over the membrane and pore blocking. In case of PES5 membrane, the value of permeability with water after the experiment was only 5% less than permeability with water before the experiment (Table S2). This means that the vibration prevented fouling and membranes used for this purpose might expect a longer lifetime. Even though PES5 gave the lowest value of permeability with water within all commercial membranes, it resulted in offering the most similar results for microalgae filtration as well as for water after experiment. Membrane performance was steady during all the time.

Permeability with water after the experiment for M5 membrane was higher than the one obtained with the virgin membrane. The explanation for this phenomenon can be the influence of membrane swelling on the pore size, resulting in increasing porosity and improvement of performance in terms of permeation.

Fig. 5 presents the permeability change with time during experiments for both microalgae filtration techniques using PES5 membrane. In the first minutes of the experiments, permeability was decreasing significantly due to primary fouling effect. However, after around 15 minutes the system was becoming stabilized and, in the case of dynamic filtration, after 20 minutes the steady state was reached. In the cross-flow filtration much more time was required to attain the plateau. Again, the cause was cake formation over the membrane surface and pore blocking, which were significantly reduced by using the vibrating set-up. Another advantage is that steady state with dynamic filtration was reached at the permeability value around 3 times higher than with the conventional method.

### 3.2.3 Initial biomass concentration effect

Another variable checked was the influence of the initial biomass concentration on dynamic filtration experiments. To assess this parameter, experiments with VSEP were performed with PES5 membrane, which corresponded to the commercial membrane giving the best performance.

Figure 6 shows permeability results of three different experiments performed with three different initial biomass concentrations as shown in figure 6. For each experiment, permeability with water before and after the experiment was measured as well as the microalgae one.

Figure 6 shows that the concentration of microalgae had a clear influence on permeability. An initial tendency was that when the initial concentration increased, permeability decreased. This can be observed comparing the first and the second experiment, with initial optical densities of 0.2 and 0.8 respectively. For these two experiments, permeability with microalgae sludge decreased 25%. Nevertheless, an interesting result was that when the initial concentration was further increased, the permeability with microalgae sludge did not significantly decrease any further. If experiments 2 and 3 are compared, permeability with microalgae sludge was around $3.0 \cdot 10^{-7}$ m $h^{-1}$ $Pa^{-1}$ while initial optical density of the sludge was 0.8 and 1.5 respectively. This means that in terms of dynamic filtration a higher concentration of feed did not contribute to more fouling generation on the membrane.

Although reaching the highest concentration was not the objective of this study, the experiments resulted in obtaining a noticeable concentration factor of 18 using the dynamic system. From an optical density of 0.2, a final one of 3.6 was achieved. As a reference, the measure was that an optical density of 0.413 is related to a microalgae ash free concentration of 0.26 g/L.

### 3.2.4 Biomass rejection

The concentrations of microalgae culture used as a feed for filtration experiments as well as concentrations of permeate and retentate were characterized by using results of optical density measurements. The total rejection of microalgae was obtained and confirmed by absorbance measurements within all the filtration experiments performed. For example, the results of the optical density measurements of *Chlorella sorokiniana* culture in dynamic filtration experiments using PES5 membrane with different concentrations of microalgae are presented in Figure 7. As was mentioned before, in this particular experiment retentate obtained from vibratory dewatering of original culture was collected and used as a feed for further experiments (Concentrated culture 1 and Concentrated culture 2). It can be observed that permeate in all cases had a similar value of OD as fresh water, which means that it was free of microalgae cells and total rejection was achieved.

## 4. CONCLUSIONS

Vibrational membrane filtration substantially improves *Chlorella sorokiniana* dewatering compared to conventional membrane cross-flow filtration. Permeability is more than doubled.

A reduction of operational cost in membrane dewatering was accomplished with the production and use of ABS membranes that were three orders of magnitude cheaper than commercial ones.

ABS membranes worked successfully in the dynamic module setup and completely rejected microalgae, which make them suitable for this application. Polymeric composition and temperature of the coagulation bath are key parameters that should be considered in the production of ABS membranes in order to obtain membranes with proper mechanical characteristics.

A first positive scale-up indicator obtained in this study is that, although there exists an initial permeability decrement when the initial biomass concentration increases, an asymptotic behavior occurs. Therefore, filtration performance may continue to be satisfactory with sludge concentration increment.

## Acknowledgements

This work was supported by the project CTQ2014-56285-R “Cultivo, concentración, fraccionamiento y obtención de producto en refinería de microalgas” funded by the Spanish Ministry of Economy and Competitiveness.

The research was also supported by the European Regional Development Funds (ERDF, FEDER Programa Competitividad de Catalunya 2007-2013).

M. Haponska is grateful to the Universitat Rovira I Virgili (URV) for her PhD scholarship.

Authors are thankful to Styrolution Europe GmbH (Frankfurt am Main, Germany) for providing the ABS material and especially to Mr. Stephan Gschwind and Mr. Udo Köster (Styrolution) for the management.

## REFERENCES

[1] E.F. Aransiola, T. V Ojumu, O.O. Oyekola, T.F. Madzimbamuto, D.I.O. Ikhu-Omoregbe, A review of current technology for biodiesel production: State of the art, Biomass Bioenerg. 61 (2014) 276–297. doi:http://dx.doi.org/10.1016/j.biombioe.2013.11.014.

[2] A.L. Ahmad, N.H.M. Yasin, C.J.C. Derek, J.K. Lim, Microalgae as a sustainable energy source for biodiesel production: A review, Renew. Sustain. Energy Rev. 15 (2011) 584–593. doi:http://dx.doi.org/10.1016/j.rser.2010.09.018.

[3] Y. Chisti, Biodiesel from microalgae, Biotechnol. Adv. 25 (2007) 294–306. doi:http://dx.doi.org/10.1016/j.biotechadv.2007.02.001.

[4] M.K. Lam, K.T. Lee, Microalgae biofuels: A critical review of issues, problems and the way forward, Biotechnol. Adv. 30 (2012) 673–690. doi:http://dx.doi.org/10.1016/j.biotechadv.2011.11.008.

[5] S.D. Ríos, J. Castañeda, C. Torras, X. Farriol, J. Salvadó, Lipid extraction methods from microalgal biomass harvested by two different paths: Screening studies toward biodiesel production, Bioresour. Technol. 133 (2013) 378–388. doi:http://dx.doi.org/10.1016/j.biortech.2013.01.093.

[6] R. Harun, M. Singh, G.M. Forde, M.K. Danquah, Bioprocess engineering of microalgae to produce a variety of consumer products, Renew. Sustain. Energy Rev. 14 (2010) 1037–1047. doi:10.1016/j.rser.2009.11.004.

[7] A. Kirrolia, N.R. Bishnoi, R. Singh, Microalgae as a boon for sustainable energy production and its future research &amp; development aspects, Renew. Sustain. Energy Rev. 20 (2013) 642–656. doi:http://dx.doi.org/10.1016/j.rser.2012.12.003.

[8] I. Rawat, R. Ranjith Kumar, T. Mutanda, F. Bux, Biodiesel from microalgae: A critical evaluation from laboratory to large scale production, Appl. Energy. 103 (2013) 444–467. doi:http://dx.doi.org/10.1016/j.apenergy.2012.10.004.

[9] N. Pragya, K.K. Pandey, P.K. Sahoo, A review on harvesting, oil extraction and biofuels production technologies from microalgae, Renew. Sustain. Energy Rev. 24 (2013) 159–171. doi:http://dx.doi.org/10.1016/j.rser.2013.03.034.

[10] S. Şirin, R. Trobajo, C. Ibanez, J. Salvadó, Harvesting the microalgae Phaeodactylum tricornutum with polyaluminum chloride, aluminium sulphate, chitosan and alkalinity-induced flocculation, J. Appl. Phycol. 24 (2012) 1067–1080. doi:10.1007/s10811-011-9736-6.

[11] T. Coward, J.G.M. Lee, G.S. Caldwell, Development of a foam flotation system for harvesting microalgae biomass, Algal Res. 2 (2013) 135–144. doi:http://dx.doi.org/10.1016/j.algal.2012.12.001.

[12] A.J. Dassey, C.S. Theegala, Harvesting economics and strategies using centrifugation for cost effective separation of microalgae cells for biodiesel applications, Bioresour. Technol. 128 (2013) 241–245. doi:http://dx.doi.org/10.1016/j.biortech.2012.10.061.

[13] P.J.L.B. Williams, L.M.L. Laurens, Microalgae as biodiesel & biomass feedstocks: Review & analysis of the biochemistry, energetics & economics, Energy Environ. Sci. 3 (2010) 554. doi:10.1039/b924978h.

[14] S.D. Ríos, C.M. Torres, C. Torras, J. Salvadó, J.M. Mateo-Sanz, L. Jiménez, Microalgae-based biodiesel: economic analysis of downstream process realistic scenarios., Bioresour. Technol. 136 (2013) 617–25. doi:10.1016/j.biortech.2013.03.046.

[15] M.R. Bilad, H.A. Arafat, I.F.J. Vankelecom, Membrane technology in microalgae cultivation and harvesting: A review, Biotechnol. Adv. 32 (2014) 1283–1300. doi:http://dx.doi.org/10.1016/j.biotechadv.2014.07.008.

[16] G. Kang, Y. Cao, Application and modification of poly(vinylidene fluoride) (PVDF) membranes – A review, J. Memb. Sci. 463 (2014) 145–165. doi:10.1016/j.memsci.2014.03.055.

[17] S.D. Rios, E. Clavero, J. Salvadó, X. Farriol, C. Torras, Dynamic Microfiltration in Microalgae Harvesting for Biodiesel Production, Ind. Eng. Chem. Res. 50 (2011) 2455–2460.

doi:10.1021/ie101070q.

[18] C. Nurra, E. Franco, M. Maspoch, J. Salvadó, C. Torras, Cheaper membrane materials for microalgae dewatering, J. Mater. Sci. 49 (2014) 7031–7039. doi:10.1007/s10853-014-8408-8.

[19] S.D. Ríos, J. Salvadó, X. Farriol, C. Torras, Antifouling microfiltration strategies to harvest microalgae for biofuel, Bioresour. Technol. 119 (2012) 406–418. doi:http://dx.doi.org/10.1016/j.biortech.2012.05.044.

[20] M.Y. Jaffrin, Dynamic shear-enhanced membrane filtration: A review of rotating disks, rotating membranes and vibrating systems, J. Memb. Sci. 324 (2008) 7–25. doi:10.1016/j.memsci.2008.06.050.

[21] W. Shi, M.M. Benjamin, Effect of shear rate on fouling in a Vibratory Shear Enhanced Processing (VSEP) RO system, J. Memb. Sci. 366 (2011) 148–157. doi:10.1016/j.memsci.2010.09.051.

[22] C. Nurra, E. Clavero, J. Salvadó, C. Torras, Vibrating membrane filtration as improved technology for microalgae dewatering, Bioresour. Technol. 157 (2014) 247–253. doi:http://dx.doi.org/10.1016/j.biortech.2014.01.115.

[23] C.S. Slater, M.J. Savelski, P. Kostetskyy, M. Johnson, Shear-enhanced microfiltration of microalgae in a vibrating membrane module, Clean Technol. Environ. Policy. (2015). doi:10.1007/s10098-015-0907-z.

[24] S. Olivera, H.B. Muralidhara, K. Venkatesh, K. Gopalakrishna, C.S. Vivek, Plating on acrylonitrile–butadiene–styrene (ABS) plastic: a review, J. Mater. Sci. 51 (2016) 3657–3674.

[25] A.M. Díez-Pascual, D. Gascón, Carbon nanotube buckypaper reinforced acrylonitrile-butadiene-styrene composites for electronic applications, ACS Appl. Mater. Interfaces. 5 (2013) 12107–12119.

[26] H. Ohno, Y. Kawamura, Analysis of acrylonitrile, 1,3-butadiene, and related compounds in acrylonitrile-butadiene-styrene copolymers for kitchen utensils and children's toys by headspace gas chromatography/mass spectrometry, J. AOAC Int. 93 (2010) 1965–1971.

[27] D.P. Cole, J.C. Riddick, H.M. Iftekhar Jaim, K.E. Strawhecker, N.E. Zander, Interfacial mechanical behavior of 3D printed ABS, J. Appl. Polym. Sci. 133 (2016) 43671. doi:10.1002/app.43671.

[28] H. Sanaeepur, A. Ebadi Amooghin, A. Moghadassi, A. Kargari, S. Moradi, D. Ghanbari, A novel acrylonitrile-butadiene-styrene/poly(ethylene glycol) membrane: preparation, characterization, and gas permeation study, Polym. Adv. Technol. 23 (2012) 1207–1218. doi:10.1002/pat.2031.

[29] A.G. Boricha, Z.V.P. Murthy, Acrylonitrile butadiene styrene/chitosan blend membranes: Preparation, characterization and performance for the separation of heavy metals, J. Memb. Sci. 339 (2009) 239–249. doi:10.1016/j.memsci.2009.04.057.

[30] S. Bandehali, A. Kargari, A. Moghadassi, H. Saneepur, D. Ghanbari, Acrylonitrile-butadiene-styrene/poly(vinyl acetate)/nanosilica mixed matrix membrane for He/CH 4 separation, Asia-Pacific J. Chem. Eng. 9 (2014) 638–644. doi:10.1002/apj.1792.

[31] J. Pruvost, G. Van Vooren, G. Cogne, J. Legrand, Investigation of biomass and lipids production with Neochloris oleoabundans in photobioreactor, Bioresour. Technol. 100 (2009) 5988–5995. doi:10.1016/j.biortech.2009.06.004.

[32] C. Torras, L. Pitol-Filho, R. Garcia-Valls, Two methods for morphological characterization of internal microcapsule structures, J. Memb. Sci. 305 (2007) 1–4. doi:10.1016/j.memsci.2007.06.056.

[33] C. Torras, R. Garcia-Valls, Quantification of membrane morphology by interpretation of scanning electron microscopy images, J. Memb. Sci. 233 (2004) 119–127. doi:10.1016/j.memsci.2003.12.016.

[34] New Logic Research, Membrane Filtration of Waste Oil Case Study. A cost-effective and environmentally sound processing solution, (2001) 1–5. http://www.vsep.com/pdf/WasteOil.pdf.

[35] R. Förch, H. Schönherr, A. Tobias, A. Jenkins, Appendix C: Contact Angle Goniometry, in:

Surf. Des. Appl. Biosci. Nanotechnol., 2009: pp. 471–473. doi:978-3-527-40789-7.

[36] X. Zhang, Q. Hu, M. Sommerfeld, E. Puruhito, Y. Chen, Harvesting algal biomass for biofuels using ultrafiltration membranes., Bioresour. Technol. 101 (2010) 5297–304. doi:10.1016/j.biortech.2010.02.007.

[37] B. Tansel, N. Dizge, I.N. Tansel, Analysis of high resolution flux data to characterize fouling profiles of membranes with different MWCO under different filtration modes, Sep. Purif. Technol. 173 (2017) 200–208. doi:10.1016/j.seppur.2016.09.032.

## Figure Captions

Fig. 1: Experimental equipment for microalgae dewatering: (a) cross-flow membrane module setup, (b) dynamic membrane module setup, adapted from [22].

Fig. 2: SEM cross-section micrographs of commercial and synthesized membranes: a) PES5, b) PAN50, c) PES20, d) M4, e) M5.

Fig. 3: Permeability results of cross-flow filtration experiments.

Fig. 4: Permeability results of dynamic filtration experiments.

Fig. 5: Permeability profiles with time for PES5 membrane in cross-flow and dynamic filtration experiments.

Fig. 6: Permeability results for the dewatering experiments with different concentrations of *Chlorella sorokiniana* culture.

Fig. 7: Optical density of *Chlorella sorokiniana* culture in dynamic filtration experiments with different concentrations of microalgae.

Table 1: **Composition of synthesized polymeric membranes.**

| Membrane | Polymer | Solvent | Concentration of polymeric solution (g polymer / 100 g total) | Non-solvent | Temperature of coagulation bath (°C, ± 5°C) |
|---|---|---|---|---|---|
| M1 | ABS | DMA | 15 | water | 20 |
| M2 | ABS | DMA | 20 | water | 20 |
| M3 | ABS | DMA | 25 | water | 20 |
| M4 | ABS | DMA | 30 | water | 20 |
| M5 | ABS | DMA | 30 | water | 50 |
| M6 | ABS | DMA | 15 | IPA/water | 20 |
| M7 | ABS | DMA | 20 | IPA/water | 20 |
| M8 | ABS | DMA | 25 | IPA/water | 20 |
| M9 | ABS | DMA | 30 | IPA/water | 20 |
| M10 | ABS | NMP | 15 | water | 20 |
| M11 | ABS | NMP | 20 | water | 20 |
| M12 | ABS | NMP | 25 | water | 20 |
| M13 | ABS | acetone | 30 | water | 20 |

Table 2: **Porosity and water contact angle values of membranes.**

| Membranes | Porosity (%) | Contact Angle (degrees) |
|---|---|---|
| *Commercial* | | |
| PES5 | 66.6 | 86.9 ± 1.1 |
| PAN50 | 63.8 | 55.1 ± 0.5 |
| PES20 | 63.2 | 89.4 ± 1.1 |
| | | |
| *Synthesized* | | |
| M4 | 37.1 | 80.7 ± 2.0 |
| M5 | 41.3 | 69.9 ± 1.1 |

Table S1: **Permeability results for conventional cross-flow filtration**

| Membranes | Permeability ($m \cdot h^{-1} Pa^{-1}$) | | |
|---|---|---|---|
| | Water before experiment | Microalgae dewatering | Water after experiment |
| *Commercial* | | | |
| PES5 | $4.8 \cdot 10^{-7} \pm 3.3 \cdot 10^{-8}$ | $1.1 \cdot 10^{-7} \pm 2.8 \cdot 10^{-8}$ | $3.8 \cdot 10^{-7} \pm 0.4 \cdot 10^{-8}$ |
| PAN50 | $2.0 \cdot 10^{-6} \pm 3.0 \cdot 10^{-8}$ | $9.7 \cdot 10^{-8} \pm 0.9 \cdot 10^{-8}$ | $1.8 \cdot 10^{-6} \pm 1.7 \cdot 10^{-7}$ |
| PES20 | $2.6 \cdot 10^{-6} \pm 1.7 \cdot 10^{-7}$ | $1.8 \cdot 10^{-7} \pm 4.4 \cdot 10^{-8}$ | $4.8 \cdot 10^{-7} \pm 3.5 \cdot 10^{-8}$ |
| *Synthesized* | | | |
| M4 | $2.9 \cdot 10^{-8} \pm 1.0 \cdot 10^{-8}$ | $1.7 \cdot 10^{-8} \pm 0.2 \cdot 10^{-8}$ | $2.0 \cdot 10^{-8} \pm 0.8 \cdot 10^{-8}$ |
| M5 | $4.0 \cdot 10^{-7} \pm 2.1 \cdot 10^{-7}$ | $4.3 \cdot 10^{-8} \pm 2.3 \cdot 10^{-8}$ | $2.6 \cdot 10^{-7} \pm 1.7 \cdot 10^{-7}$ |

Table S2: **Permeability results for dynamic filtration**

| Membranes | Permeability ($m \cdot h^{-1} Pa^{-1}$) | | |
|---|---|---|---|
| | Water before experiment | Microalgae dewatering | Water after experiment |
| *Commercial* | | | |
| PES5 | $4.7 \cdot 10^{-7} \pm 6.0 \cdot 10^{-8}$ | $4.2 \cdot 10^{-7} \pm 5.0 \cdot 10^{-8}$ | $4.4 \cdot 10^{-7} \pm 5.8 \cdot 10^{-8}$ |
| PAN50 | $1.6 \cdot 10^{-6} \pm 1.6 \cdot 10^{-7}$ | $3.2 \cdot 10^{-7} \pm 5.2 \cdot 10^{-8}$ | $7.2 \cdot 10^{-7} \pm 3.8 \cdot 10^{-7}$ |
| PES20 | $1.2 \cdot 10^{-6} \pm 9.4 \cdot 10^{-8}$ | $3.5 \cdot 10^{-7} \pm 3.4 \cdot 10^{-8}$ | $4.9 \cdot 10^{-7} \pm 0.6 \cdot 10^{-8}$ |
| *Synthesized* | | | |
| M5 | $1.0 \cdot 10^{-7} \pm 3.8 \cdot 10^{-8}$ | $6.6 \cdot 10^{-8} \pm 3.2 \cdot 10^{-8}$ | $1.4 \cdot 10^{-7} \pm 6.0 \cdot 10^{-8}$ |

Figure 01

Click here to download high resolution image

a) **Tangential cross-flow membrane module setup**

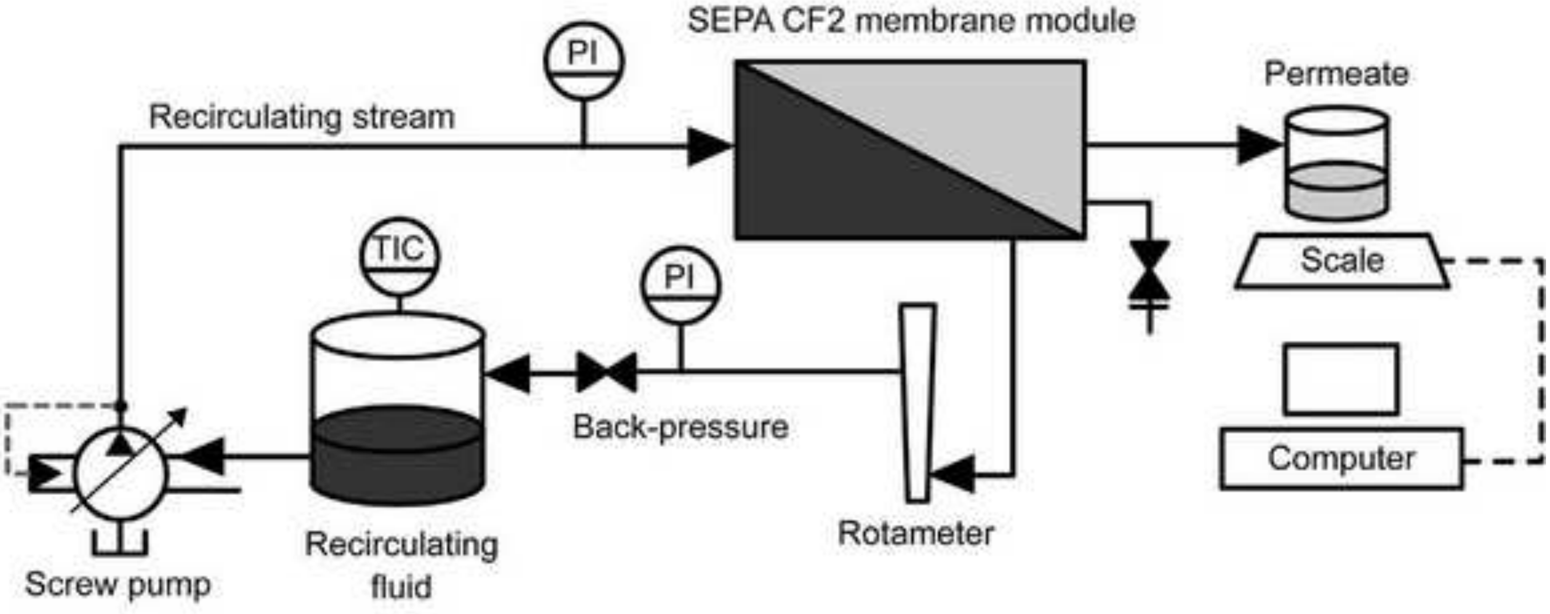

b) **Dynamic membrane module setup**

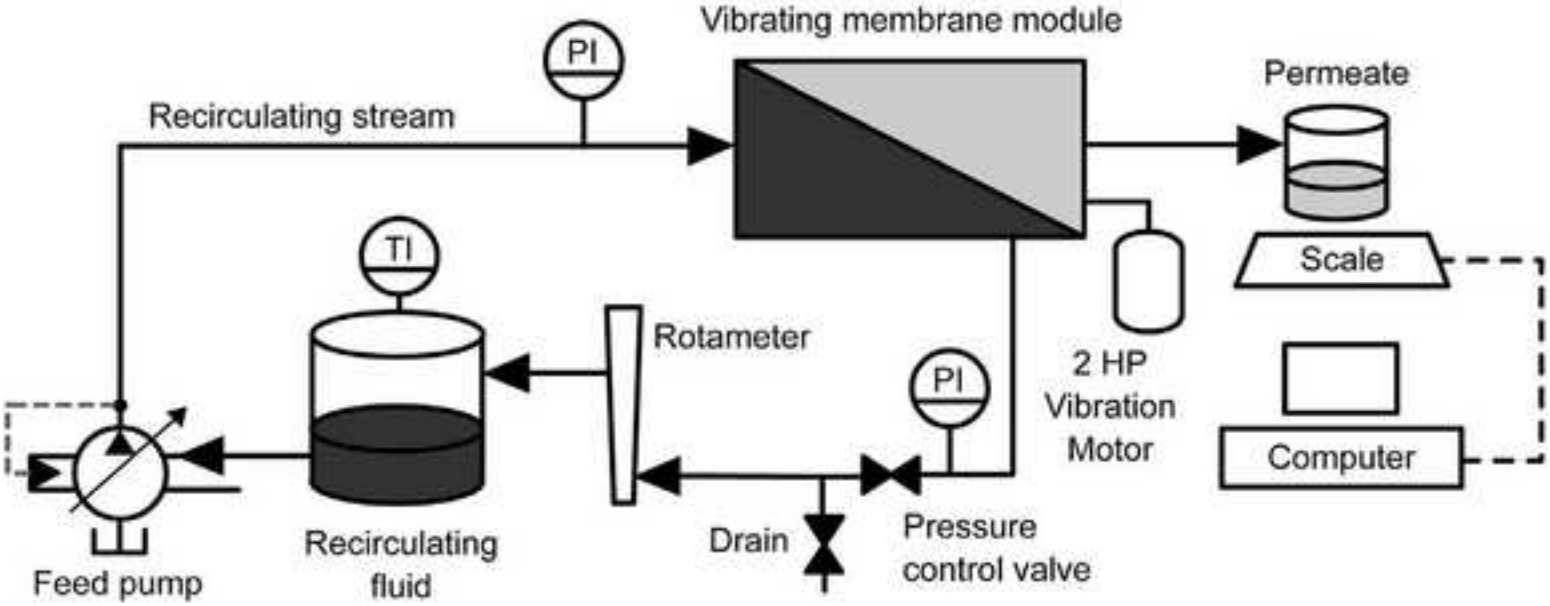

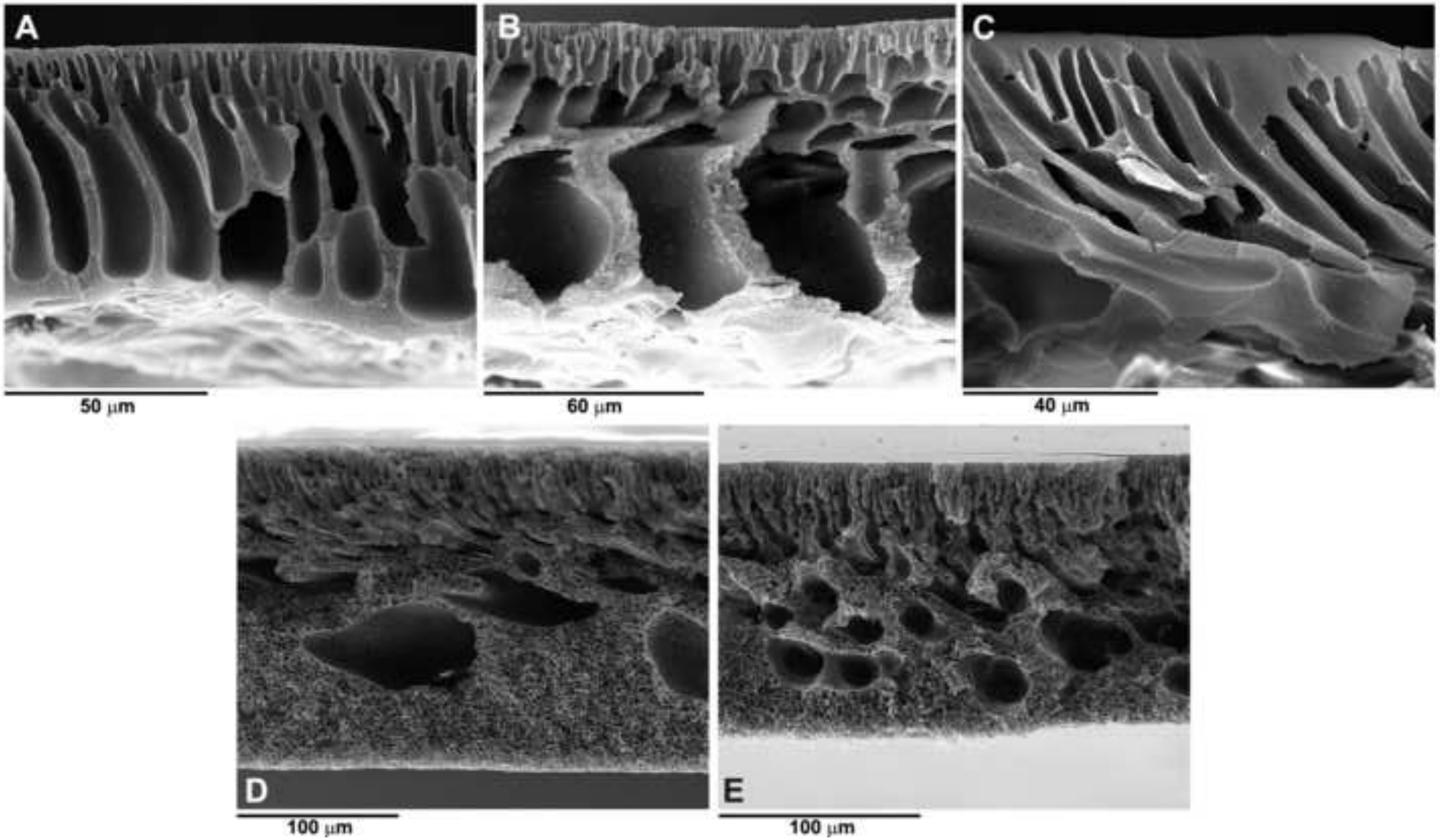
A
B
C
50 µm
60 µm
40 µm
D
E
100 µm
100 µm

**Figure 03**

**Click here to download high resolution image**

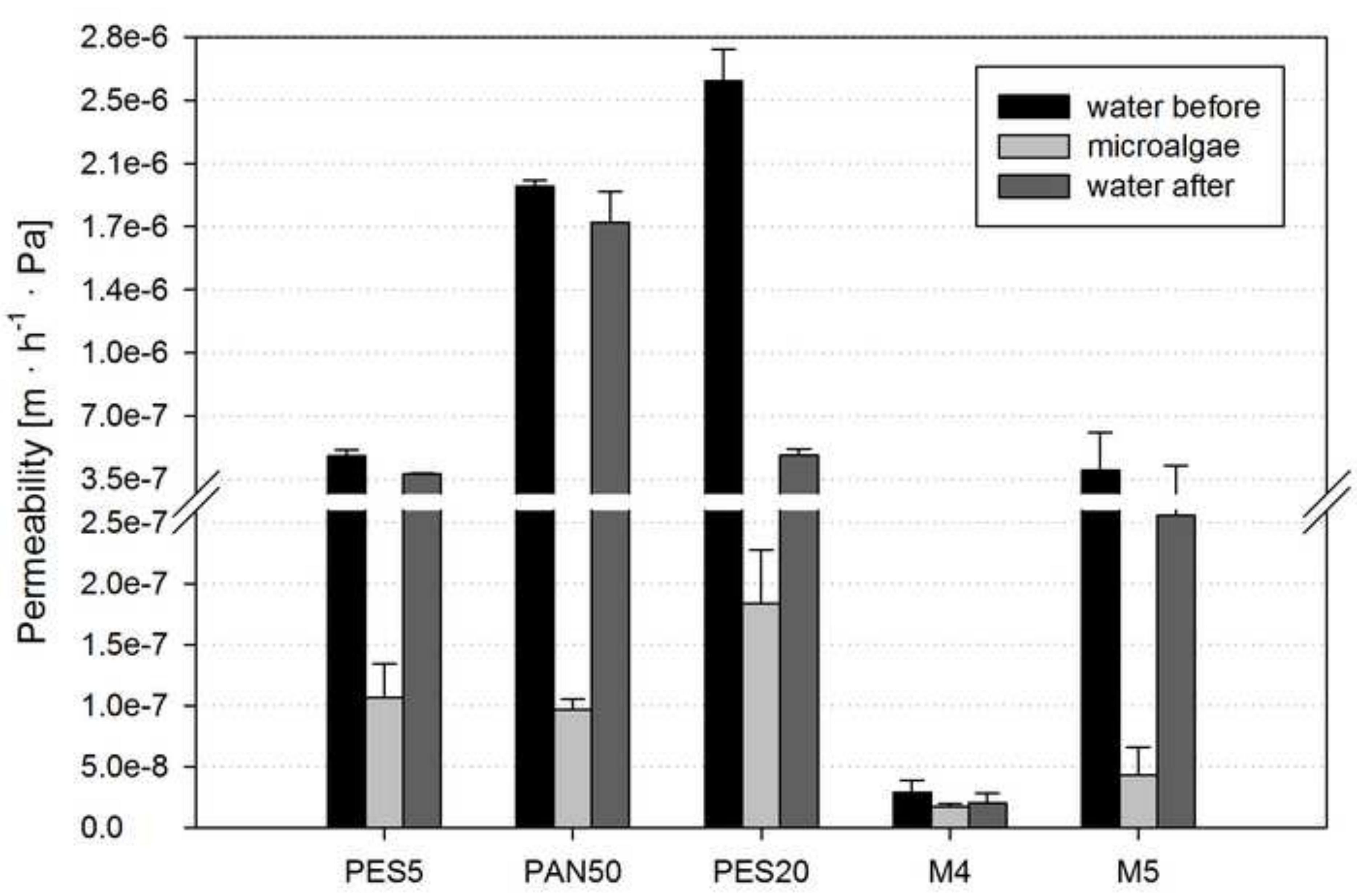

Figure 04

Click here to download high resolution image

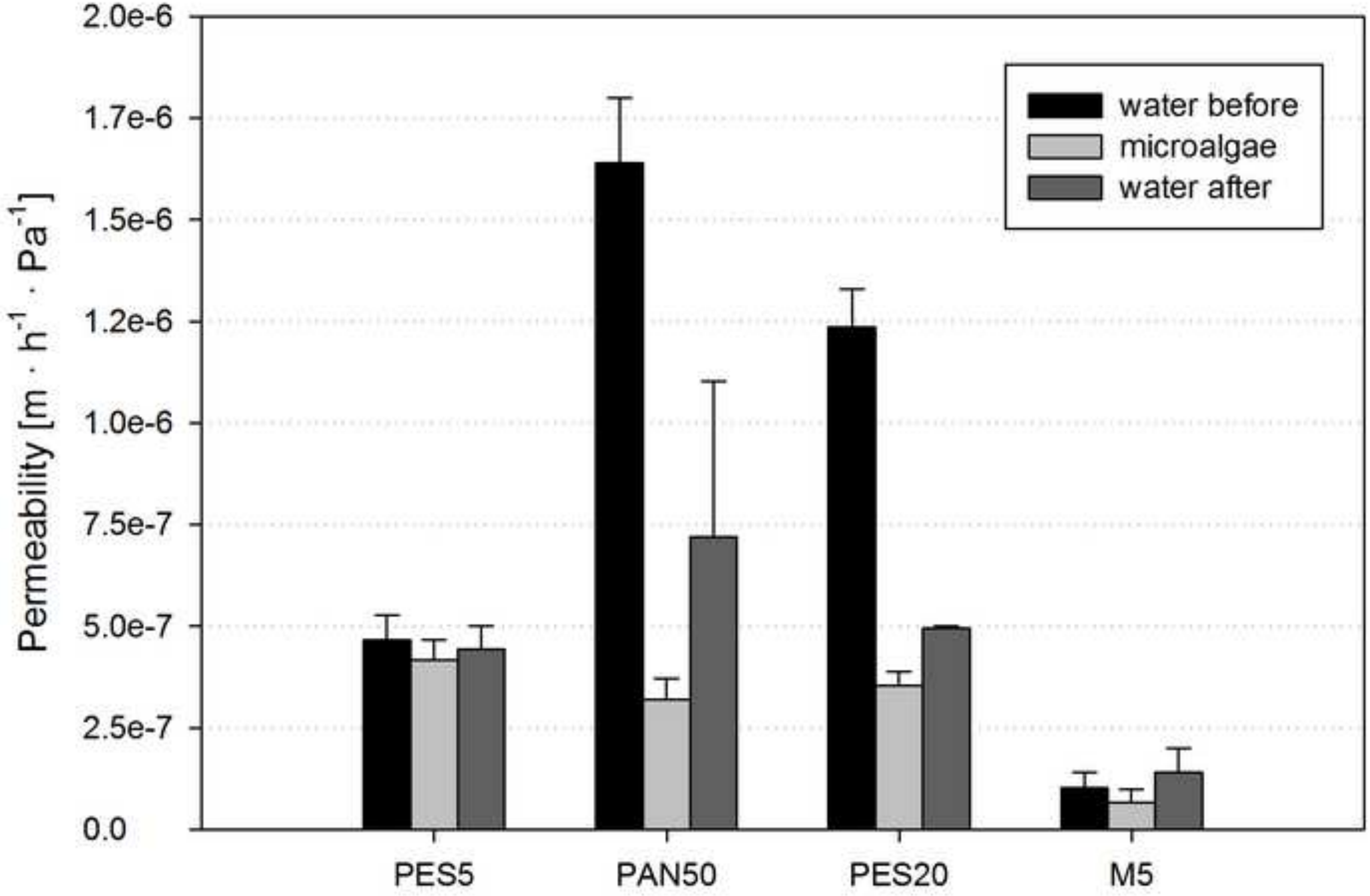

**Figure 05**

**Click here to download high resolution image**

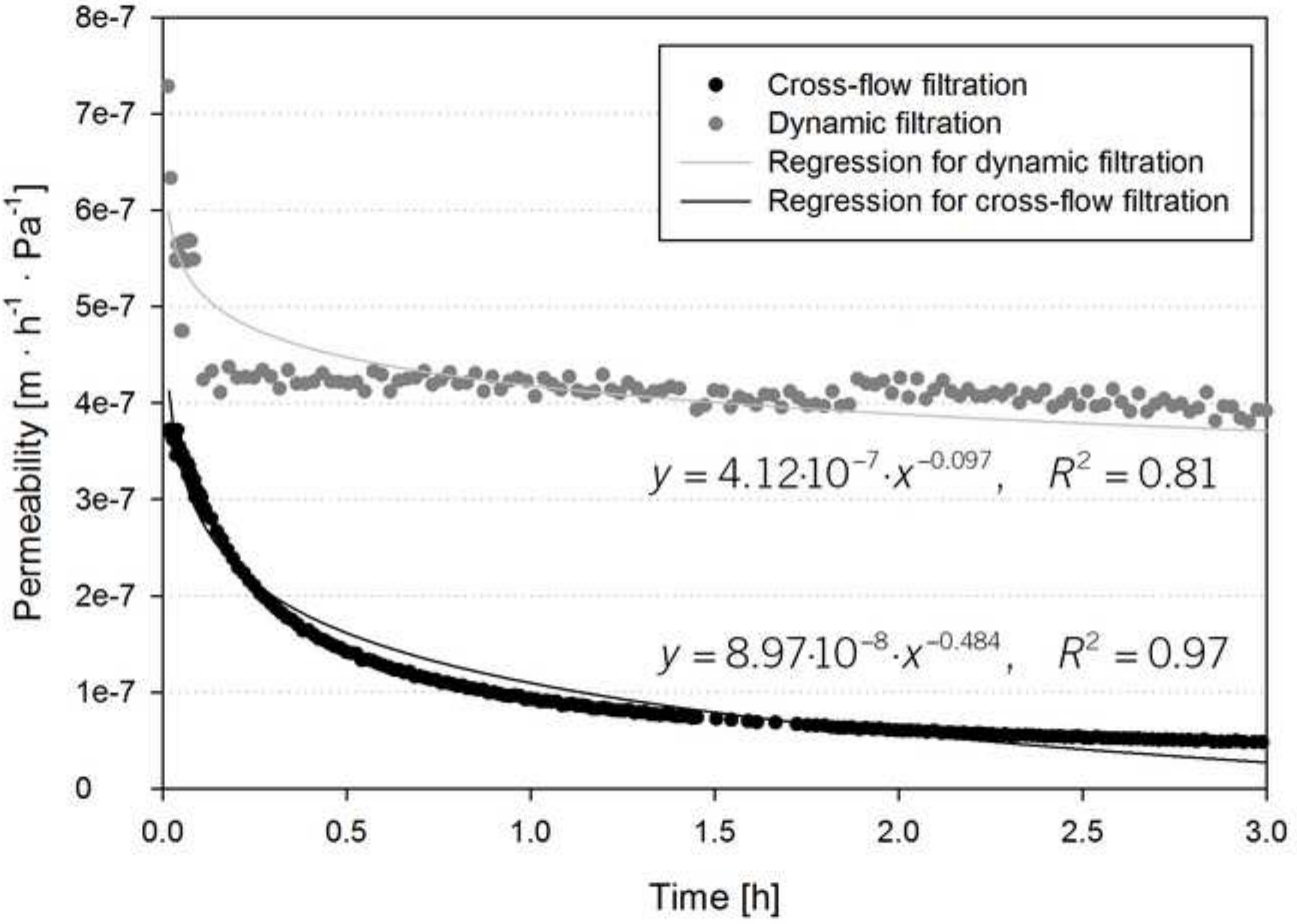

**Figure 06**

Click here to download high resolution image

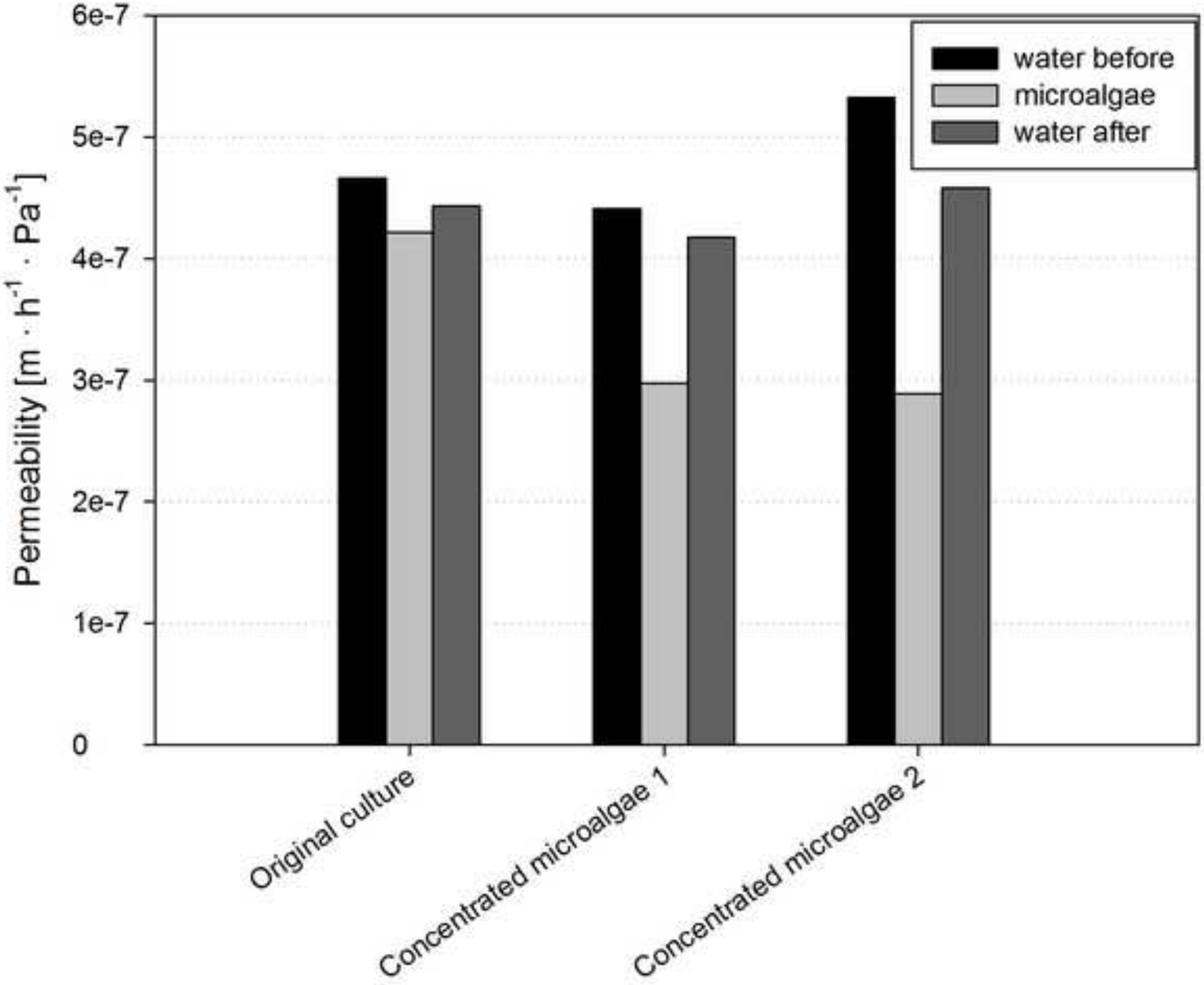

**Figure 07**

Click here to download high resolution image